Viscous incompressible flow between concentric rotating spheres. Part 1. Basic flow

By B. R. MUNSON

Department of Mechanical Engineering, Duke University, Durham, North Carolina

AND D. D. JOSEPH

Department of Aerospace Engineering and Mechanics,
University of Minnesota, Minneapolis, Minnesota

The steady motion of a viscous fluid contained between two concentric spheres which rotate about a common axis with different angular velocities is considered. A high-order analytic perturbation solution, through terms of order Re^7, is obtained for low Reynolds numbers. For larger Reynolds numbers an approximate Legendre polynomial series representation is used to reduce the governing system of equations to a non-linear ordinary differential equation boundary-value problem which is solved numerically. The resulting flow pattern and the torque required to rotate the spheres are presented for various cases considered.

1. Introduction

We consider here the steady laminar motion of an incompressible viscous fluid contained between two concentric spheres which rotate about a common axis with fixed angular velocities. This spherical annulus flow is a special example of fluid motion in a rotating container and is of interest in both engineering design and geophysics. In part 2 we consider the hydrodynamic stability of the steady laminar motion discussed here.

Since we consider rotationally symmetric flows (independent of the longitude) the governing incompressible Navier–Stokes equations take the form of a pair of coupled non-linear partial differential equations, one fourth order and the other second order, in terms of a meridian plane stream function and an angular velocity function. These equations are solved in terms of a high-order analytic perturbation solution in powers of the Reynolds number, Re, for small or moderate values of Re. For larger values of Re the partial differential equations are written as an infinite set of coupled non-linear ordinary differential equations by means of a Legendre polynomial expansion of the dependent variables. An appropriate truncation of the expansion provides a finite-order non-linear two-point ordinary differential equation boundary-value problem which is integrated numerically. This Galerkin-type procedure allows the flow field to be determined at Reynolds numbers larger than those obtainable by the perturbation solution.

Previous theoretical work concerning the flow in a spherical annulus can be grouped as either (i) low-order analytic perturbation solutions for small Reynolds numbers, (ii) singular perturbation considerations (boundary layer-inviscid

core) for large Reynolds numbers and (iii) numerical integration of the governing partial differential equations. For example, Ovseenko (1963) has shown that for sufficiently small Re the flow of a viscous incompressible fluid within a specified volume can be obtained in the form of an analytic perturbation solution in terms of a power series in Re. He determined this solution for a specific case of a spherical annulus through terms of order Re^3. Higher-order terms, necessary in order to consider larger values of Re, were not obtained because of the rapid increase in complexity of the governing system as the order is increased. One objective of this study is to determine the higher-order perturbation solution.

For large Reynolds numbers singular perturbation solutions have been considered by various authors including Proudman (1956), Stewartson (1966), Pedlosky (1969), Carrier (1965), Bondi & Lyttleton (1948) and others. Pearson (1967) has integrated the time-dependent governing partial differential equations numerically to determine the flow field for several cases with Reynolds numbers from 10 to 1000.

Thus except for Pearson's results the previous considerations appear to be limited to either very small or very large Reynolds numbers – in either case the Reynolds numbers are not in the range needed in the stability analysis of part 2. In addition, the relatively large computational time necessary to numerically integrate the partial differential equations and the resulting form of the solution (values at various mesh points) are not well suited for use in a stability analysis.

Hence we determine the basic flow for moderate values of Re in terms of a high-order analytic perturbation solution (through terms of order Re^7 for example) and also in terms of an appropriate series truncation (actually a Galerkin-type procedure). In addition to the flow field considerations we consider the torque required to rotate the spheres at their given angular velocities.

2. Governing equations

The geometry of the spherical annulus considered is indicated in figure 1. A viscous incompressible fluid fills the gap between the inner and outer spheres which are of radii R_1 and R_2 and rotate about a common axis with constant angular velocities Ω_1 and Ω_2, respectively. Since the flow is assumed to be independent of the longitude, ϕ, the Navier–Stokes equations can be written in terms of a stream function in the meridian plane, ψ, and an angular velocity function, Ω, as follows (Rosenhead 1963):

$$
\left.
\begin{aligned}
-\frac{\psi_r \Omega_\theta - \psi_\theta \Omega_r}{r^2 \sin\theta} &= \frac{1}{Re}\tilde{D}^2\Omega, \\[2mm]
\frac{2\Omega}{r^3\sin^2\theta}[\Omega_r r\cos\theta - \Omega_\theta\sin\theta] &- \frac{1}{r^2\sin\theta}[\psi_r(\tilde{D}^2\psi)_\theta - \psi_\theta(\tilde{D}^2\psi)_r] \\[2mm]
+\frac{2\tilde{D}^2\psi}{r^3\sin^2\theta}[\psi_r r\cos\theta - \psi_\theta\sin\theta] &= \frac{1}{Re}\tilde{D}^4\psi,
\end{aligned}
\right\}
\tag{1}
$$

where
$$
\left.
\begin{aligned}
\tilde{D}^2 &= \frac{\partial^2}{\partial r^2} + \frac{1}{r^2}\frac{\partial^2}{\partial\theta^2} - \frac{1}{r^2}\cot\theta\frac{\partial}{\partial\theta}, \\[2mm]
( )_r &= \partial/\partial r, \quad ( )_\theta = \partial/\partial\theta.
\end{aligned}
\right\}
\tag{2}
$$

The non-dimensional velocities are related to ψ and Ω as follows

$$v_r = \frac{\partial\psi/\partial\theta}{r^2\sin\theta}, \quad v_\theta = \frac{-\partial\psi/\partial r}{r\sin\theta}, \quad v_\phi = \frac{\Omega}{r\sin\theta},$$

where r is the dimensionless radial co-ordinate. The Reynolds number is defined by

$$Re = \Omega_0 R_2^2/\nu \tag{3}$$

where R_2 is taken as the characteristic length and Ω_0 as the characteristic angular velocity. In the two extreme cases, $\Omega_0 = \Omega_1$ if the outer sphere is stationary and
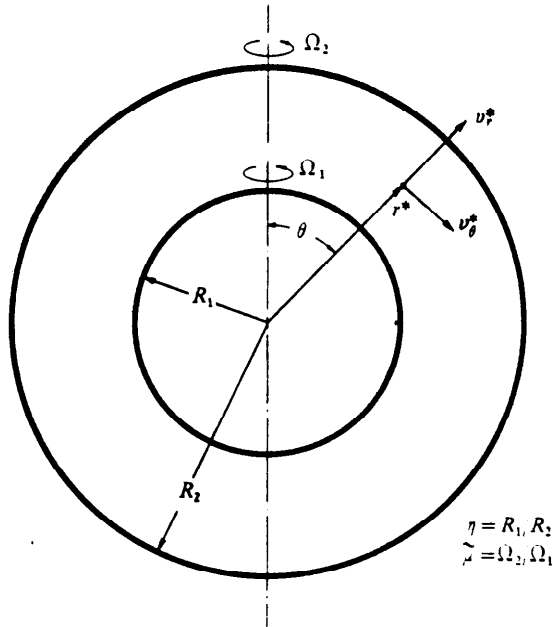

FIGURE 1. Spherical annulus.

$\Omega_0 = \Omega_2$ if the inner sphere is stationary. When both spheres rotate the character of the flow field is generally dominated by the motion of either the inner or outer sphere. The angular velocity of the dominant sphere is then taken as the characteristic angular velocity. The specific choice of Ω_0 is indicated for each example considered. The flow is assumed to be symmetric with respect to the equator so that the range of the independent variables becomes

$$\eta \leqslant r \leqslant 1, \quad 0 \leqslant \theta \leqslant \tfrac{1}{2}\pi,$$

where $\eta = R_1/R_2$ is the radius ratio. Change to the physical variables, denoted by ( )*, is accomplished according to

$$^*r = R_2 r, \quad \psi^* = R_2^3\Omega_0\psi, \quad \Omega^* = R_2^2\Omega_0\Omega,$$

$$v_r^* = \frac{\partial\psi^*/\partial\theta}{r^{*2}\sin\theta}, \quad v_\theta^* = \frac{-\partial\psi^*/\partial r^*}{r^*\sin\theta}, \quad v_\phi^* = \frac{\Omega^*}{r^*\sin\theta}.$$

The viscous boundary conditions which complete the formulation of the problem are that $\psi = \partial\psi/\partial n = 0$ on the boundaries, with n denoting the unit normal, and Ω is prescribed since the angular velocities are given.

Thus the fluid motion consists of a 'primary motion' about the axis of rotation given by Ω and a 'secondary motion' in the meridian plane given by ψ. Although the secondary motion is small relative to the motion about the axis of rotation when the Reynolds number is small, it can become comparable to the primary motion for larger values of Reynolds number.

3. Perturbation solution for low or moderate Reynolds numbers

In this section we consider a high-order analytic perturbation solution of the above system which governs the viscous incompressible flow in a spherical annulus. As indicated previously, Ovseenko (1963) has shown that for sufficiently small Reynolds numbers the flow in a bounded region, such as a spherical annulus, can be obtained in the form of an analytic perturbation solution in positive powers of Re. Ovseenko considered such a solution but because of the difficulties in the mechanics of calculating the vast number of coefficients needed for the high-order solutions he limited his considerations to terms of order Re^3 or less. As shown below, the use of a computer as an accurate book-keeping device allows the perturbation solution to be carried out to a high order.

In order to obtain a solution valid for larger Reynolds numbers we consider here the results through Re^7. In principle we can calculate all of the Taylor coefficients for the perturbation solution, but in practice accuracy in determining these coefficients limits the order of the perturbation solution which can be obtained. Thus, it turns out, we are limited to values of Re less than 100 or so, and it is not possible to determine the radius of convergence of the perturbation solution (either analytically or numerically). It is not ruled out that the solution may be an entire function in Re.

The perturbation solution of equations (1) can be written in the form

$$
\left.
\begin{aligned}
\psi(r, \theta) &= \sum_{\substack{l=1 \\ \text{odd}}}^{\infty} Re^l \left[\sum_{\substack{j=1 \\ \text{odd}}}^{l} \sin^2\theta P_j(\theta) g_{jl}(r) \right], \\
\Omega(r, \theta) &= \sum_{\substack{l=0 \\ \text{even}}}^{\infty} Re^l \left[\sum_{\substack{j=0 \\ \text{even}}}^{l} \sin^2\theta P_j(\theta) f_{jl}(r) \right],
\end{aligned}
\right\}
\tag{4}
$$

where $P_j(\theta)$ is the jth-order Legendre polynomial. Thus the θ dependence of ψ and Ω separates from the r dependence for the perturbation solution and allows the governing system to be written as an ordinary differential equation problem for the component functions $f_{jl}(r)$, $g_{jl}(r)$. This set of equations is obtained by substitution of the form given by (4) into the governing equations (1) and equating like powers of Re. The θ dependence is removed by multiplying the system by an appropriate Legendre polynomial, $P_m(\theta)$, and integrating over $0 \leqslant \theta \leqslant \pi$. Use of various orthogonality properties and recurrence relations for Legendre

polynomials provide, after lengthy calculations, that the perturbation equations can be written as

$$
\mathscr{L}_n f_{np} = \frac{2(2n+1)}{r^2} \sum_{\substack{l=n+2 \\ \text{even}}}^{p} f_{lp} + (1-\delta_{p0}) \frac{(2n+1)}{2r^2} \sum_{l=0}^{p-1} \sum_{m=\max[0,\,n-l-1]}^{p-1-l} \sum_{j=l}^{\min[p-1-m,\,p-1]}
$$

$$
\times \left[a_{lmn} g_{lj} f'_{m,\,p-j-1} - a_{mln} g'_{lj} f_{m,\,p-j-1} \right] \quad \text{for} \quad n = 0, 2, 4, \ldots
$$

$$
\text{and} \quad p = 0, 2, 4, \ldots, n,
$$

and

$$
L_n g_{np} = \frac{4(2n+1)}{r^2} \sum_{\substack{l=n+2 \\ \text{odd}}}^{p} M_l g_{lp} + \frac{(2n+1)}{2r^3} \sum_{l=0}^{p-1} \sum_{m=\max[0,\,n-l-1]}^{p-1-l} \sum_{j=l}^{\min[p-1-m,\,p-1]}
$$

$$
\times \left[(A_{lmn} r f'_{lj} + B_{lmn} f_{lj}) f_{m,\,p-j-1} + (C_{lmn} r g'''_{lj} \right.
$$

$$
+ E_{lmn} g''_{lj} + F_{lmn} \frac{1}{r} g'_{lj} + G_{lmn} \frac{1}{r^2} g_{lj}) g_{m,\,p-j-1}
$$

$$
+ D_{lmn} r g''_{lj} g'_{m,\,p-j-1} \right] \quad \text{for} \quad n = 1, 3, 5, \, , \ldots \quad \text{and} \quad p = 1, 3, 5, \ldots, n,
$$

where

$$
(\ )' \equiv d/dr.
$$

$$(5)$$

The operators $\mathscr{L}_n,\, L_n,\, M_l$ are defined as

$$
\begin{aligned}
\mathscr{L}_n &= \frac{d^2}{dr^2} - \frac{(n+1)(n+2)}{r^2}, \\
L_n &= \frac{d^4}{dr^4} + \frac{a_n}{r^2} \frac{d^2}{dr^2} + \frac{b_n}{r^3} \frac{d}{dr} + \frac{c_n}{r^4}, \\
M_l &= \frac{d^2}{dr^2} - \frac{2}{r} \frac{d}{dr} + \frac{[2 - l(l+1)]}{r^2},
\end{aligned}
\qquad (6)
$$

where

$$
a_n = -2(n+1)(n+2), \quad b_n = 4(n+1)(n+2),
$$

$$
c_n = (n-1)(n+2)(n+1)(n+4)
$$

and δ_{p0} is the Kronecker delta. The boundary conditions corresponding to (5) become

$$
\begin{aligned}
g_{lm} = g'_{lm} = 0 \quad &\text{at} \quad r = \eta, \quad r = 1 \quad \text{for all} \quad l, m, \\
f_{lm} = 0 \quad &\text{at} \quad r = \eta, \quad r = 1 \quad \text{for all} \quad l, m \neq 0, 0,
\end{aligned}
$$

and either

$$
f_{00} = \eta^2/\tilde{\mu} \quad \text{at} \quad r = \eta \quad \text{and} \quad f_{00} = 1 \quad \text{at} \quad r = 1 \quad \text{if} \quad Re = \Omega_2 R_2^2/\nu,
$$

or

$$
f_{00} = \eta^2 \quad \text{at} \quad r = \eta \quad \text{and} \quad f_{00} = \tilde{\mu} \quad \text{at} \quad r = 1 \quad \text{if} \quad Re = \Omega_1 R_2^2/\nu,
$$

$$(7)$$

where $\tilde{\mu} = \Omega_2/\Omega_1$ is the angular velocity ratio. The numerous constants

$$
a_{lmn}, \quad A_{lmn}, \quad B_{lmn}, \quad \ldots, \quad G_{lmn}
$$

are defined in terms of integrals of various combinations of Legendre polynomials, their derivatives, and trigonometric functions. These constants can all be evaluated either explicitly or in terms of recurrence formulas in terms of the single integral,

$$
N_{pqs} \equiv \int_{-1}^{1} P_q P_p P_s \, dx, \quad x = \cos\theta,
$$

given by Hobson (1955, p. 87). The detailed evaluation of these constants can be obtained from Munson (1970).

The component functions, $f_{np}(r)$, $g_{np}(r)$, are solved successively as

$$f_{00}, g_{11}, f_{22}, f_{02}, g_{33}, g_{13}, f_{44}, \ldots$$

up to the desired order. When solving successively in this fashion the governing equations are of the form

$$\left. \begin{array}{c} \mathscr{L}_n f_{np}(r) = \mathscr{F}(r), \\ L_n g_{np}(r) = \mathscr{G}(r), \end{array} \right\} \tag{8}$$

where $\mathscr{F}(r)$, $\mathscr{G}(r)$ are functions known in terms of the previously calculated lower order f_{ij}, g_{ij}. The solutions of these inhomogeneous equations are given by

$$f_{np}(r) = \frac{1}{(2n+3)} \int_\eta^r [r^{n+2}\xi^{-(n+1)} - r^{-(n+1)}\xi^{n+2}] \mathscr{F}(\xi) \, d\xi + \tilde{A}r^{-(n+1)} + \tilde{B}r^{(n+2)}, \tag{9}$$

and

$$g_{np}(r) = \frac{1}{2(2n+3)} \int_\eta^r \left[\frac{1}{(2n+5)} (r^{n+4}\xi^{-(n+1)} - r^{-(n+1)}\xi^{n+4}) \right.$$

$$\left. + \frac{1}{(2n+1)} (r^{1-n}\xi^{n+2} - r^{n+2}\xi^{1-n}) \right] \mathscr{G}(\xi) \, d\xi + Ar^{n+4} + Br^{n+2} + Cr^{1-n} + Dr^{-(1+n)}, \tag{10}$$

where the constants $\tilde{A}$, $\tilde{B}$, A, B, C, D, are determined such that the desired boundary conditions are satisfied at $r = \eta$ and $r = 1$.

Careful consideration of the governing equations (5) and the solutions of the inhomogeneous equations (9), (10) combined with the fact that either multiplication, differentiation or integration of the function $r^i(\ln r)^j$, where i, j are integers, will produce a function of the same form shows that the desired solution can be written as

$$f_{np}(r) = \sum_i \sum_j \alpha_{np}^{ij} r^i (\ln r)^j, \quad g_{np}(r) = \sum_i \sum_j \beta_{np}^{ij} r^i (\ln r)^j. \tag{11}$$

Here the integer i ranges over an appropriate interval (both positive and negative) and j is a non-negative integer. The problem, then, is to determine these coefficients α_{np}^{ij}, β_{np}^{ij} such that the perturbation equations and boundary conditions are satisfied. The large number of coefficients involved in the higher-order solutions (on the order of one thousand coefficients for a solution through Re^7) and the great accuracy needed for these coefficients dictate the use of the computer as an accurate book-keeping device.

For a given radius ratio, $\eta = R_1/R_2$, and a given angular velocity ratio, $\tilde{\mu} = \Omega_2/\Omega_1$, the actual solution to the perturbation problem is carried out as follows. We start with the lowest-order function, $f_{00}(r)$, and calculate the solution through the desired order as indicated previously. Hence with the lower-order solutions known by previous calculation the right-hand side of (5) is determined in the form

$$f_{np} = \sum_i \sum_j \tilde{\alpha}_{np}^{ij} r^i (\ln r)^j, \quad g_{np} = \sum_i \sum_j \tilde{\beta}_{np}^{ij} r^i (\ln r)^j,$$

where the coefficients $\tilde{\alpha}_{np}^{ij}$, $\tilde{\beta}_{np}^{ij}$ and the range of the indices are kept track of by the computer. The solution of the inhomogeneous equations (9), (10) are deter-

mined in a similar form and the appropriate boundary conditions are applied to determine the various otherwise arbitrary constants in (9), (10).

We compare here the various order perturbation solutions at various Reynolds numbers with the solutions calculated by a Galerkin-type procedure discussed in the next section. In particular we consider the results as a function of the radial co-ordinate r for $\theta = 45°$ at various values of Re for the case where $\eta = 0.5$ and $\tilde{\mu} = \infty$; that is the inner sphere half the diameter of the outer sphere and the inner sphere not rotating. These results are typical for other values of r, θ, η and $\tilde{\mu}$. Figures 2 and 3 indicate the results.
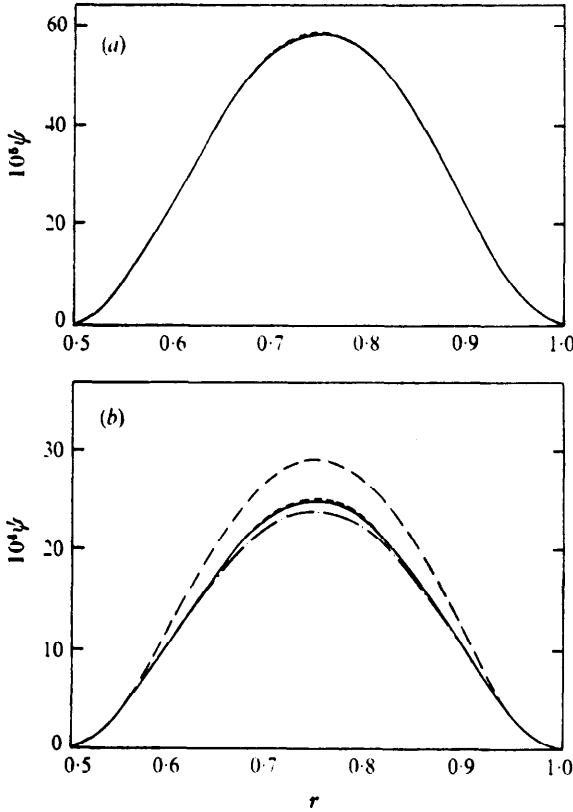
FIGURE 2. Comparison of stream function, ψ, for various order perturbation solutions with (a) $Re = 10$ and (b) $Re = 50$. $\theta = 45°$, $\eta = 0.5$, $\tilde{\mu} = \infty$. Perturbation order N_p: ———, 1; —·—, 3; ———, 5; ———, true solution.

Previous considerations have been limited to either the lowest-order terms (through Re) or at most through Re^3. For $Re < 10$ these low-order solutions and the true solutions are essentially the same, but for $Re = 50$ the lowest-order solution is in error by about 20 %. However, the fifth-order solution (through Re^5) agrees very well with the actual solution for $Re = 50$ (about 1 % difference). For $Re = 80$ even the seventh-order solution is in error by about 15 %, but as the order increases the perturbation solutions appears to be converging to the true solution.

Although for $Re = 100$ the perturbation solution appears to diverge it is not known if the radius of convergence is in the neighbourhood of $Re = 100$ or if the apparent divergence is caused by insufficient accuracy in calculating the numerous coefficients of the exact perturbation solution. The latter is felt to be the case.
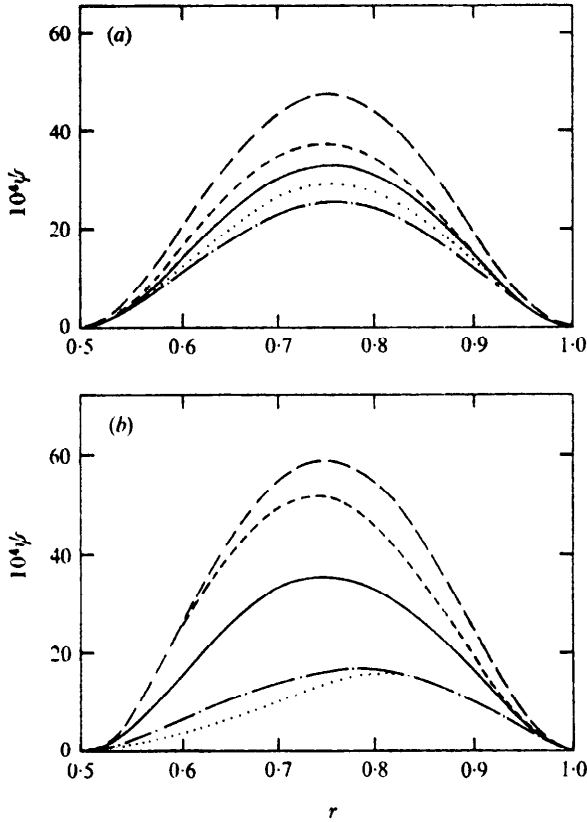

FIGURE 3. Comparison of stream function, ψ, for various order perturbation solutions with (a) $Re = 80$ and (b) $Re = 100$. $\theta = 45°$, $\eta = 0.5$, $\bar{\mu} = \infty$. Perturbation order N_p: —— , 1; —·— , 3; — — — , 5; · · · , 7; —— , true solution.

It is not uncommon for the fourteen-place computer accuracy to be insufficient for problems of this type which consist of solutions containing many terms, as is the case for the higher-order solutions. In fact such accuracy problems did not allow the perturbation solution to be carried out through terms of higher order than Re^7.

Although it would be of interest to know the exact radius of convergence (or to have an approximate rigorous estimate), the complexities of the governing equations apparently have not allowed this as yet. It is not ruled out that the perturbation solution may be an entire function in Re. In any event, the inclusion of terms of order greater than Re^3 is seen to provide a fairly accurate description of the flow field for Reynolds numbers considerably above the $Re = 10$ limit of the low-order consideration.

4. Legendre polynomial series representation

Since the analytic perturbation solution discussed above did not allow the solution to be calculated at Reynolds numbers large enough for the stability considerations of part 2 the following method was used. The functions ψ, Ω can be expanded in a Legendre polynomial series representation as

$$\begin{aligned}
\psi(r,\theta) &= \sum_{l=0}^{\infty} \sin^2\theta P_l(\theta)\, g_l(r), \\
\Omega(r,\theta) &= \sum_{l=0}^{\infty} \sin^2\theta P_l(\theta)\, f_l(r),
\end{aligned} \right\} \tag{12}$$

where the non-linear ordinary differential equations governing the component functions $f_l(r)$, $g_l(r)$ can be obtained from the original system (1). Of course the result is an infinite set of coupled equations. An appropriate truncation of the series given in (12) thus results in a finite number of coupled ordinary differential equations which can be integrated numerically. Essentially the method is an appropriate Galerkin-type procedure used to reduce the original partial differential equation to ordinary differential equations. That the method works well with the series truncated at a reasonable value will be seen below.

Two advantages of solving the original problem in this fashion as opposed to a numerical integration of the original partial differential equations are the following. For a given physical system (given Re, η, $\tilde{\mu}$) the computer time necessary to generate a solution in terms of the Legendre polynomial expansion is less than that required to integrate the original partial differential equations. Secondly, the results in terms of numerical values for the r dependence and Legendre polynomial representation for the θ dependence are more convenient for the stability considerations than a set of values of ψ, Ω at various mesh points throughout the r and θ range.

Thus the functions ψ, Ω are truncated as

$$\begin{aligned}
\psi(r,\theta) &= \sum_{\substack{l=1 \\ \text{odd}}}^{N_t} \sin^2\theta P_l(\theta)\, g_l(r), \\
\Omega(r,\theta) &= \sum_{\substack{l=0 \\ \text{even}}}^{N_t} \sin^2\theta P_l(\theta)\, f_l(r),
\end{aligned} \right\} \tag{13}$$

and substituted into (1). Multiplication by $P_n(\theta)$ and integration over $0 \leqslant \theta \leqslant \pi$ (similar to what was done for the perturbation equations (5)) produces the following set of coupled non-linear ordinary differential equations.

$$\mathscr{L}_n f_n - \frac{2(2n+1)}{r^2} \sum_{\substack{l \geqslant n+2 \\ \text{even}}} f_l = \frac{(2n+1)}{2} \frac{Re}{r^2} \sum_l \sum_{\substack{m \\ l+m>n-2}} a_{lmn}(g_l f_m' - g_m' f_l), \tag{14}$$

for $\quad n = 0, 2, \ldots, N_t - 1,$

and $\quad L_n g_n - \dfrac{4(2n+1)}{r^2} \displaystyle\sum_{\substack{l \geqslant n+2 \\ \text{odd}}} M_l g_l = \dfrac{2n+1}{2} \dfrac{Re}{r^3} \displaystyle\sum_l \sum_{\substack{m \\ l+m>n-2}} \Bigg(A_{lmn} r f_l' f_m$

$$+ B_{lmn} f_l f_m + C_{lmn} r g_l''' g_m + D_{lmn} r g_l'' g_m' + E_{lmn} g_l'' g_m$$

$$+ F_{lmn} \frac{1}{r} g_l' g_m + G_{lmn} \frac{1}{r^2} g_l g_m \Bigg) \quad \text{for} \quad n = 1, 3, \ldots, N_t. \tag{15}$$

The various constants $a_{lmn}, A_{lmn}, \ldots, G_{lmn}$ and operators $\mathscr{L}_n, L_n, M_l$ are as-defined in §3, and the boundary conditions can be written in the following form

$$f_l = 0 \quad \text{at} \quad r = \eta, \quad r = 1 \quad \text{for} \quad l = 2, 4, \ldots, N_t - 1,$$

$$g_l = g_l' = 0 \quad \text{at} \quad r = \eta, \quad r = 1 \quad \text{for} \quad l = 1, 3, \ldots, N_t,$$

and either

$$\left. \begin{array}{l} f_0 = \eta^2 \tilde{\mu}^{-1} \quad \text{at} \quad r = \eta \\ f_0 = 1 \quad \text{at} \quad r = 1 \quad \text{if} \quad Re = R_2^2 \Omega_2 / \nu \end{array} \right\} \tag{16}$$

or

$$f_0 = \eta^2 \quad \text{at} \quad r = \eta,$$

$$f_0 = \tilde{\mu} \quad \text{at} \quad r = 1 \quad \text{if} \quad Re = R_2^2 \Omega_1 / \nu.$$

We have used the fact, which results from the assumed symmetry with respect to the equator, that $f_l(r) \equiv g_m(r) \equiv 0$ if l is odd or m is even.

To illustrate the structure of this system we consider the lowest-order truncation, $N_t = 1$ and obtain the approximation

$$\psi(r, \theta) = \sin^2 \theta \cos \theta g_1(r),$$

$$\Omega(r, \theta) = \sin^2 \theta f_0(r),$$

with the governing equations given by

$$\left. \begin{array}{l} f_0'' - \dfrac{2}{r^2} f_0 = -\dfrac{2Re}{3r^2} g_1' f_0, \\[2mm] g_1''' - \dfrac{12}{r^2} g_1' + \dfrac{24}{r^3} g_1 = \dfrac{2Re}{5r^3} \left[5 f_0 \left(r f_0' - 2 f_0 \right) + 2 r g_1 g_1''' + \left(r g_1' - 4 g_1 \right) g_1'' - \dfrac{18}{r} g_1 g_1' + \dfrac{48}{r^2} g_1^2 \right], \end{array} \right\} \tag{17}$$

and boundary conditions for a stationary inner sphere ($\tilde{\mu} = \infty$) as

$$f_0 = g_1 = g_1' = 0 \quad \text{at} \quad r = \eta,$$

$$f_0 = 1, \quad g_1 = g_1' = 0 \quad \text{at} \quad r = 1.$$

The accuracy of this representation (the lowest-order Galerkin approximation) is not expected to be good for any but small Reynolds numbers. (It is noted that a linearization of (17) is precisely the lowest-order perturbation system.) Higher-order truncations, $N_t > 1$ allowing consideration of larger Re, provide the same general form for the governing system, but the number of terms involved increases very rapidly with N_t.

The governing non-linear two-point boundary-value problem was integrated numerically using a Runge–Kutta–Gill technique for various combinations of Reynolds number, radius ratio, angular velocity ratio, at various truncation orders, N_t. For small Re the solutions obtained were compared with the perturbation solution of the previous section and for larger Re they were compared with Pearson's (1967) numerical results. In general a value of $N_t = 7$ was sufficient to provide an accurate representation of the flow field for Reynolds numbers needed in the stability considerations, $Re \leqslant 500$. It is noted that because of the extreme sensitivity to initial conditions the standard 'shooting method' could not be used in solving this boundary-value problem for $Re > 200$. For larger values of Re the quasi-linearization or Newton–Kantorovitch method was used quite successfully.

Typical results obtained by the above method are discussed below. For $Re \leqslant 10$ the lowest-order approximation, $N_t = 1$, provides a very accurate description of the flow field (as does any higher-order truncation). For $Re = 100$ and $\eta = 0.5$, $\bar{\mu} = \infty$ (inner sphere stationary), for example, the results with $N_t = 5$ are indistinguishable from those given by Pearson and the higher-order truncations.
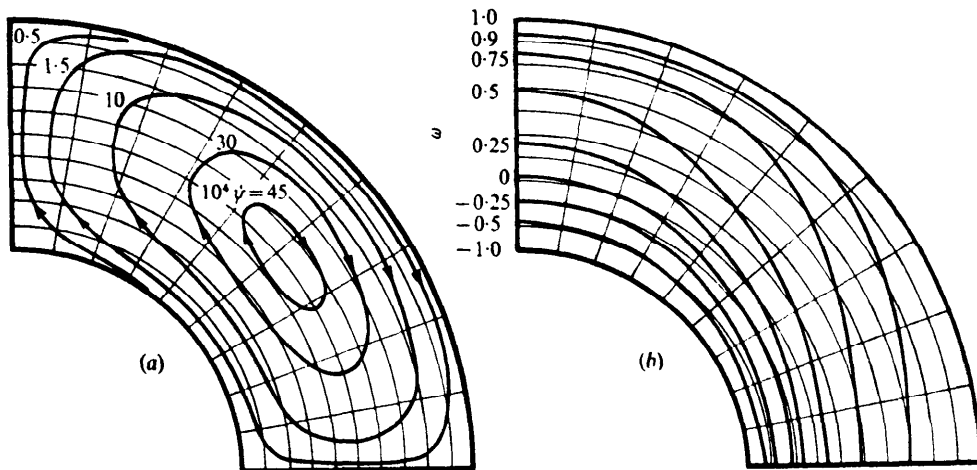

FIGURE 4. (a) Stream function, ψ, and (b) angular velocity, ω, for both spheres rotating at the same rate but in opposite directions, $\bar{\mu} = -1.0$, and $\eta = 0.5$ and $Re = \Omega_2 R_2^2/\nu = 100$.
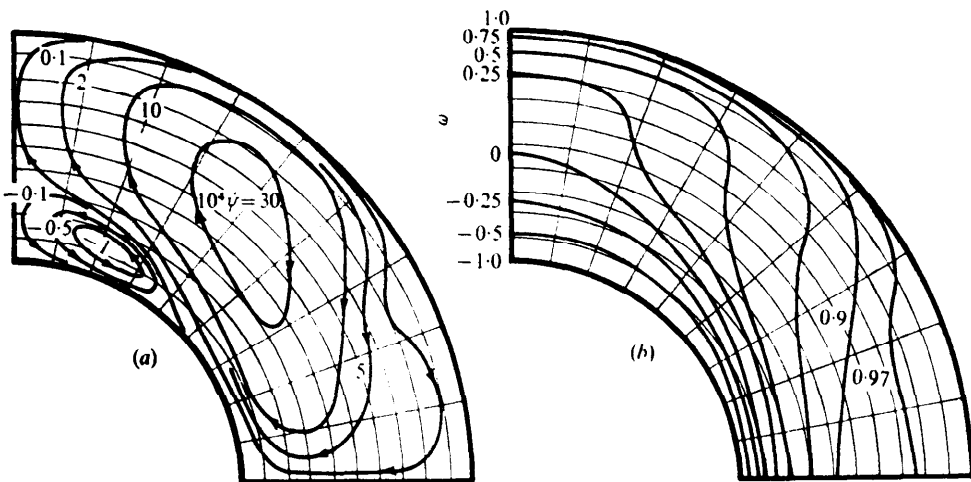
FIGURE 5. (a) Stream function, ψ, and (b) angular velocity, ω, for both spheres rotating at the same rate but in opposite directions, $\bar{\mu} = -1.0$, and $\eta = 0.5$, $Re = \Omega_2 R_2^2/\nu = 500$.

However for $Re = 1000$ and $N_t = 7$ the comparison between Pearson's solution (figures 4 and 5 of his paper) and our solution is not as good. While the angular velocity contours compare very well, the small reverse flow region near the equator is not sufficiently described by the $N_t = 7$ approximation. However for $Re \leqslant 500$ a comparison of the results for various truncations indicate that the solution with $N_t = 7$ is quite good.

The character of the flow field depends strongly on the relative rates of rotation of the two spheres. For example, with the outer sphere stationary the secondary flow consists of one counterclockwise swirl. An increase in Re increases the strength of this swirl and forces its centre closer to the equator. On the other hand,
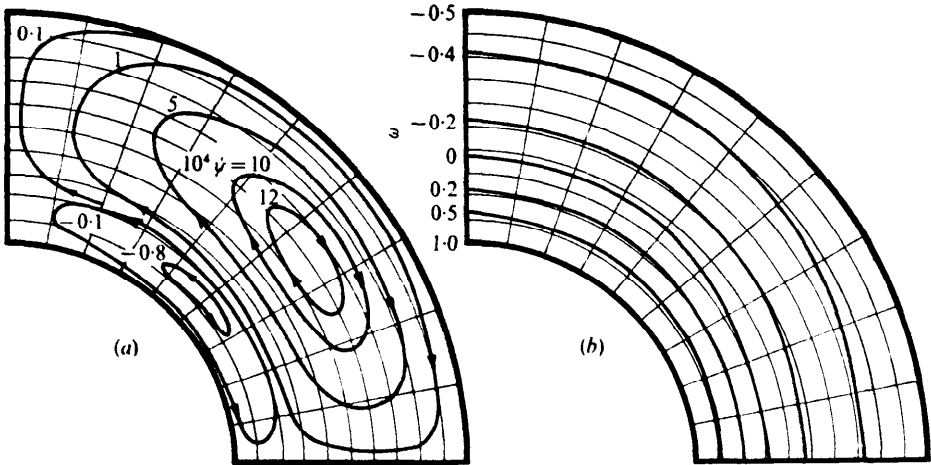

FIGURE 6. (a) Stream function, ψ, and (b) angular velocity, ω, for outer sphere rotating at half the rate of the inner sphere and in the opposite directions, $\bar{\mu} = -0.5$, and $\eta = 0.5$, $Re = \Omega_1 R_2^2/\nu = 100$.
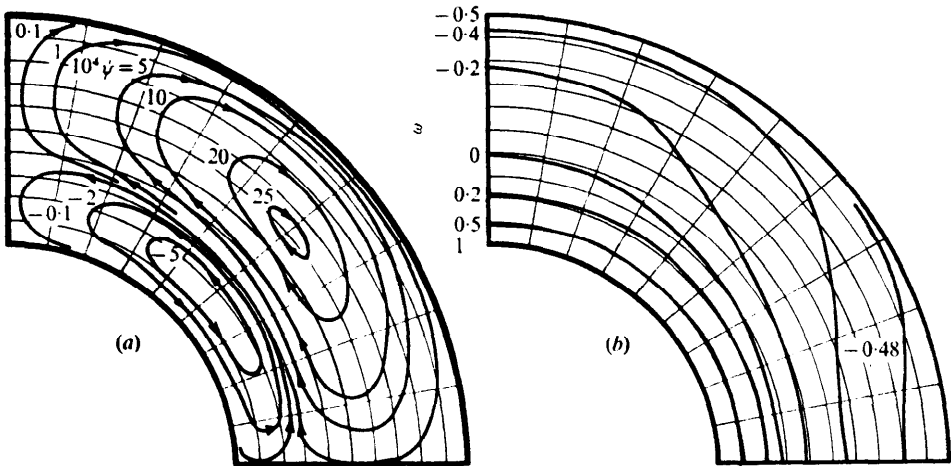
FIGURE 7. (a) Stream function, ψ, and (b) angular velocity, ω, for outer sphere rotating at half the rate of the inner sphere and in the opposite direction, $\bar{\mu} = -0.5$, and $\eta = 0.5$, $Re = \Omega_1 R_2^2/\nu = 500$.

if the inner sphere is stationary the secondary motion consists of a single clockwise swirl if Re is not too large. An increase in Re causes the flow to form a smaller counterclockwise swirl and to take on the cylindrical sheath character discussed by Proudman (1956). These characteristics are indicated by the results of Pearson (1967) and by the solutions obtained by the above method.

It is of interest to determine what flow situation prevails when both spheres rotate, but in opposite directions. Figures 4 to 7 indicate the flow field for two cases; (i) both spheres rotate at the same rate but in opposite directions, $\tilde{\mu} = -1$, and (ii) the inner sphere rotates at twice the rate of the outer sphere and in the opposite direction, $\tilde{\mu} = -0.5$. In the second case with $\eta = 0.5$ the speeds on the two spheres at the equator are equal.

As can be seen in figures 4 and 5 the motion of the outer sphere dominates when $\tilde{\mu} = -1$ with the resulting flow consisting of one clockwise swirl for $Re = 100$. The influence of the inner sphere is apparent for $Re = 500$ in terms of a small counterclockwise swirl in the polar region near the inner sphere. The tendency toward a cylindrical sheath character as Re increases is also apparent in the angular velocity contours.

As can be seen in figures 6 and 7 neither sphere dominates the flow field when $\tilde{\mu} = -0.5$. Rather two swirls of opposite direction are obtained for all values of Re considered. Again, as Re increases, the tendency toward a cylindrical sheath character is apparent (unlike the case when the outer sphere is stationary, $\tilde{\mu} = 0$). Additional results for other angular velocity and radius ratios are given by Munson (1970).

5. Torque calculations

One of the important physical properties obtainable from the basic flow discussed above is the torque required to rotate the sphere at a given rate. The torque, M, is given by

$$M = 2 \int_{\phi=0}^{2\pi} \int_{\theta=0}^{\frac{1}{2}\pi} \mu r^3 \sin^2 \theta \tau_{\phi r} d\theta d\phi,$$

where μ is the viscosity of the fluid and $\tau_{\phi r}$ the component of the stress tensor. Substitution of the Legendre polynomial expansion (12) into this expression leads to the following,

$$M = 4\pi\mu \frac{r^4 \Omega_0}{R_2} \sum_l (f_l/r^2)'|_{r=r^*/R_2} \hat{a}_l,$$

where

$$\hat{a}_l = \int_0^{\frac{1}{2}\pi} P_l(\theta) \sin^3 \theta d\theta.$$

Only the first two component functions, f_0, f_2, contribute to the sum; the remainder are zero because of the orthogonality properties of $P_l(\theta)$ (i.e. $\hat{a}_l = 0$ if l is even and $l \geqslant 4$). Thus we obtain the torque as

$$M = \tfrac{8}{3}\pi\mu\Omega_0 R_2^3 \tilde{m}, \left.\begin{array}{c} \\ \\ \end{array}\right\}$$

where
$$\tilde{m} = |(f_0' - 0.2f_2') - 2(f_0 - 0.2f_2)|_{r=1}. \quad (18)$$

Here $\tilde{m}$ is the non-dimensional torque which is a function of the geometry, η, relative rates of rotation, $\tilde{\mu}$, and Reynolds number. Figures 8 and 9 indicate this torque for four cases of interest.
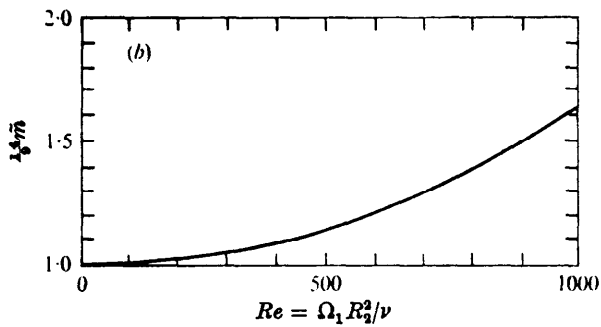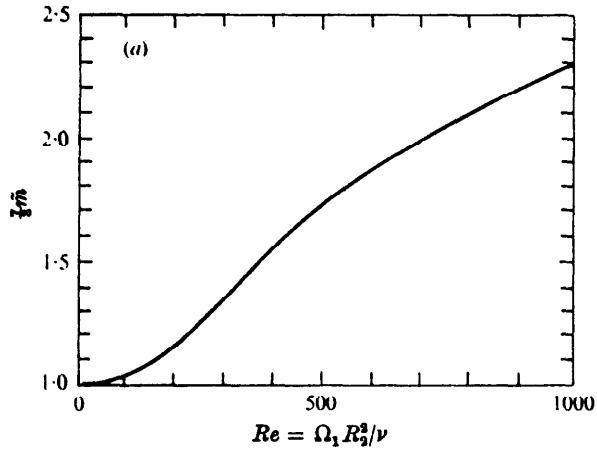
FIGURE 8. Non-dimensional torque, $\tilde{m}$, as a function of Reynolds number for rotating spheres. $\eta = 0.5$. (a) $\bar{\mu} = 0$, (b) $\bar{\mu} = -0.5$.
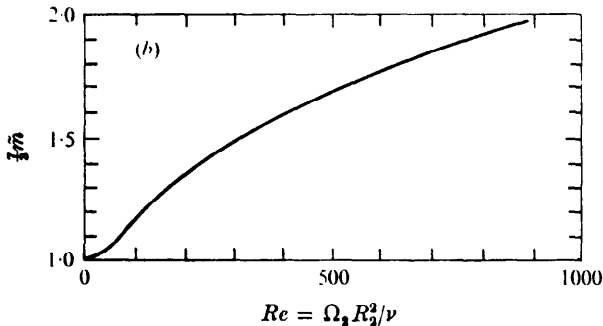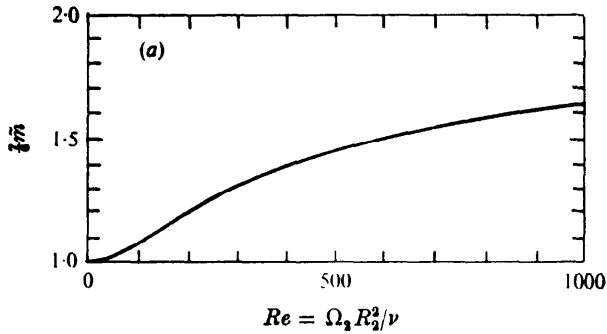

FIGURE 9. Non-dimensional torque $\tilde{m}$, as a function of Reynolds number for rotating spheres. $\eta = 0.5$. (a) $\bar{\mu} = -1$, (b) $\bar{\mu} = \infty$.

REFERENCES

BONDI, H. & LYTTLETON, R. A. 1948 On the dynamical theory of the rotation of the earth. *Proc. Camb. Phil. Soc.* **44**, 345.

CARRIER, G. F. 1965 Some effects of stratification and geometry in rotating fluids. *J. Fluid Mech.* **23**, 145.

HOBSON, E. W. 1955 *The Theory of Spherical and Ellipsoidal Harmonics*. Chelsea Pub. Co.

MUNSON, B. R. 1970 Hydrodynamic stability of flow between rotating spheres and rotating sliding cylinders. Ph.D. Thesis, University of Minnesota.

OVSEENKO, IU. G. 1963 O dvizheri viazkoi zhidkasti mezhdu dvumia urashchaiushimisia sferami (On the motion of a viscous liquid between two rotating spheres). *Izv. Vyssh. Ucheb. Zaved., Matematika*, no. 4, 129.

PEARSON, C. E. 1967 A numerical study of the time-dependent viscous flow between two rotating spheres. *J. Fluid Mech.* **28**, 323.

PEDLOSKY, J. 1969 Axially symmetric motion of a stratified, rotating fluid in a spherical annulus of narrow gap. *J. Fluid Mech.* **36**, 1969.

PROUDMAN, I. 1956 The almost-rigid rotation of viscous fluid between concentric spheres. *J. Fluid Mech.* **1**, 505.

ROSENHEAD, L. 1963 *Laminar Boundary Layers*. Oxford University Press.

STEWARTSON, K. 1966 On almost rigid rotations: Part 2. *J. Fluid Mech.* **26**, 131.